

Switchable magnetic dipole induced guided vortex motion

N. Verellen,¹ A. V. Silhanek,^{1,a)} W. Gillijns,¹ V. V. Moshchalkov,¹ V. Metlushko,²
F. Gozzini,² and B. Ilic³

¹*Nanoscale Superconductivity and Magnetism and Pulsed Fields Group, Institute for Nanoscale Physics and Chemistry (INPAC), K. U. Leuven Celestijnenlaan 200 D, B-3001 Leuven, Belgium*

²*Department of Electrical and Computer Engineering, University of Illinois, Chicago, Illinois 60607, USA*

³*Cornell Nanofabrication Facility, School of Applied and Engineering Physics, Cornell University, Ithaca, New York 14853, USA*

(Received 26 March 2008; accepted 15 June 2008; published online 16 July 2008)

We present evidence of magnetically controlled vortex motion in an Al film on top of a periodic array of Permalloy square rings. The resulting magnetic template generates a strongly anisotropic pinning potential landscape for vortices in the superconducting layer. Transport measurements show that this anisotropy is able to confine the flux motion along the high symmetry axes of the square lattice of dipoles. This guided vortex motion can be rerouted by 90° simply changing the dipole orientation or even suppressed by inducing a flux-closure magnetic state with very low stray fields in the rings. © 2008 American Institute of Physics. [DOI: 10.1063/1.2955824]

For the past years there has been a considerable effort to conceive and realize new superconducting devices that allow to modulate locally the magnetic field.¹ These systems rely essentially on static arrays of pinning centers which influence the vortex dynamics.^{2–5} The ultimate motivation behind the manipulation of the local vortex density is to enhance the performance of superconductor-based devices by reducing the noise in superconducting quantum interference based systems,^{6,7} gaining control on superconducting terahertz emitters⁸ or even providing a way to predefine the optical transmission through the system.⁹

Unfortunately, for the majority of the components used in fluxonics devices, once they are created there is no margin for further modifications. In some cases this lack of flexibility becomes a limiting factor in the performance of the devices. For instance, a predefined ratchet system designed to effectively remove vortices from a specific location can work properly at low fields but ignores the inevitable reversed ratchet at higher fields, thus making its functionality rather impractical.^{5,10} A way to circumvent this shortcoming can be worked out by introducing magnetic pinning centers which have additional internal degrees of freedom not available in conventional nanostructured pinning sites.

In this work we demonstrate that reversible and switchable guidance of the vortex motion can be achieved using a square array of magnetic square rings lying underneath a superconducting film. Transport measurements unambiguously show that the vortex dynamics is fully dominated by the magnetic field distribution generated by the ring structures. When the magnetic unit cell is rotated 45° off the Lorentz force \mathbf{F}_L the average vortex velocity \mathbf{v} follows the direction of the principal axis of the magnetic lattice rather than the driving force. This channeling effect can be easily suppressed when inducing a nearly isotropic pinning landscape by setting the square rings in a flux-closure state with very low stray fields.

The sample used for this investigation consists of a 50 nm thick Al film evaporated on top of a checker-board array of Permalloy square rings with a lateral size of 1 μm , linewidth of 150 nm, and thickness of 25 nm [Fig. 1(a)]. The

magnetic template is electrically separated from the superconducting film by a 5 nm Si buffer layer added to reduce proximity effects.¹¹ The ring-shaped patterns and the transport bridge were fabricated with electron-beam lithography and lift-off technique on a silicon substrate. Standard Hall transport geometry with alignment of transverse voltage contacts better than half a micron and bridge width of 120 μm was used [Fig. 1(c)]. The superconducting critical temperature at zero field for the sample in the dipolar state (i.e., maximum stray field) is $T_c = 1.356$ K.

It has been shown recently that multiply connected magnetic structures can be readily switched between different magnetic states.^{12,13} For the particular square geometry chosen in this work, an in-plane external field along the diagonal of the squares can induce six different domain distributions,¹⁴ namely, four dipolar states (onion states) obtained at remanence after saturation and two flux-closure states (vortex states) with opposite chirality when the field is reduced from saturation to ± 36 mT and then set to zero. Interestingly, when these rings are placed in close proximity to a superconducting layer, either a strong vortex pinning or weak pinning can be obtained by simply switching from dipolar to flux-closure state, respectively. Although the influence of these magnetic templates on the vortex pinning is relatively well understood,¹⁵ little is known about their influence on the vortex dynamics.

In order to address this issue we carried out transport measurements recording simultaneously the electric field parallel (E_{xx}) and perpendicular (E_{xy}) to the external current. This allows us to estimate the direction α (see Fig. 1) of the average vortex motion \mathbf{v} with respect to the Lorentz force \mathbf{F}_L . A representative set of experimental data for different magnetic states of the square rings is shown in Fig. 2 at $T/T_c = 0.89$. Figure 2(a) shows the electric field-current-density (E - J) characteristic for the case when the squares have been set in the onion state magnetized 45° away from the current direction [see inset in panel (a)] and setting an out-of-plane field $H/H_1 = 1.2$, where $H_1 = \Phi_0/d^2$, with Φ_0 the flux quantum and d the period of the lattice. From Fig. 2(a) it can be seen that for low enough currents ($J < 8$ MA/cm²) the vortex lattice remains pinned as no dissipation is detected in either direction ($E_{xx} = E_{xy} \sim 0$). Surprisingly, for currents higher

^{a)}Electronic mail: alejandro.silhanek@fys.kuleuven.be.

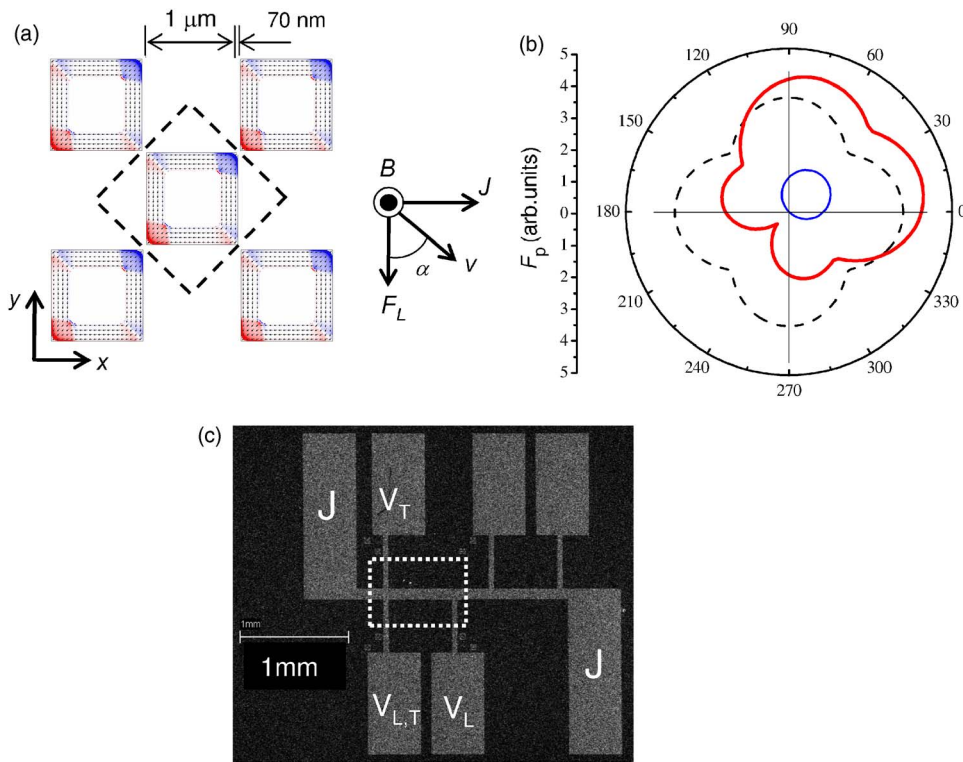


FIG. 1. (Color online) (a) Micromagnetic simulation of the out-of-plane component of the stray field at remanence for the sample investigated after applying a saturation field along their diagonal (onion state). The thick broken line indicates the magnetic unit cell. The orientation of the external current (J), field (B), driving force (F_L), and vortex drift (v) is clearly indicated. (b) Polar plot of the pinning force F_p for a test vortex located at a pinning site only considering the lattice symmetry (broken line), or the local magnetic pinning force (off-centered circle), and including both the lattice and the local symmetry (thick solid line). The angle is defined anticlockwise from the positive x -axis corresponding to the situation in panel (a). (c) SEM image of a transport bridge with current contacts J and longitudinal and transverse voltage contacts, V_L and V_T , respectively showing the measurement configuration. The dashed box contains the magnetic template.

than the critical current the direction of vortex motion does not coincide with the Lorentz force. More specifically since $E_{xx} \approx E_{xy}$ vortices move at an angle $\alpha = 45^\circ$ as indicated in the inset of Fig. 2(a). This is a clear evidence that the net displacement of the vortices is along the high symmetry axis of the magnetic pinning landscape indicated with a dashed line in Fig. 1(a). Essentially this effect is the result of an anisotropic depinning force F_{dp} which reaches its maximum F_{dp}^\perp (minimum F_{dp}^\parallel) value perpendicular (parallel) to the channel direction defined by the principal axes of the magnetic landscape. In Fig. 2(a), since the applied force is in this case 45° away from the channel direction, the critical

current J_{c1} at which vortices start moving is determined by the condition $J_{c1} = F_{dp}^\parallel \sin(45^\circ) / \Phi_o$. This situation persists up to $J_{c2} \sim 25$ MA/cm² where E_{xy} and E_{xx} gradually separate from each other which means that now the component of the Lorentz force perpendicular to the channels is large enough to overcome F_{dp}^\perp , i.e., $J_{c2} = F_{dp}^\perp \cos(45^\circ) / \Phi_o$, and vortices flow along the direction of the Lorentz force. This allows us to estimate the ratio of depinning forces as $F_{dp}^\perp / F_{dp}^\parallel = J_{c2} / J_{c1} \sim 3$.

By keeping a constant current density and progressively increasing the applied field it is possible to realize the same

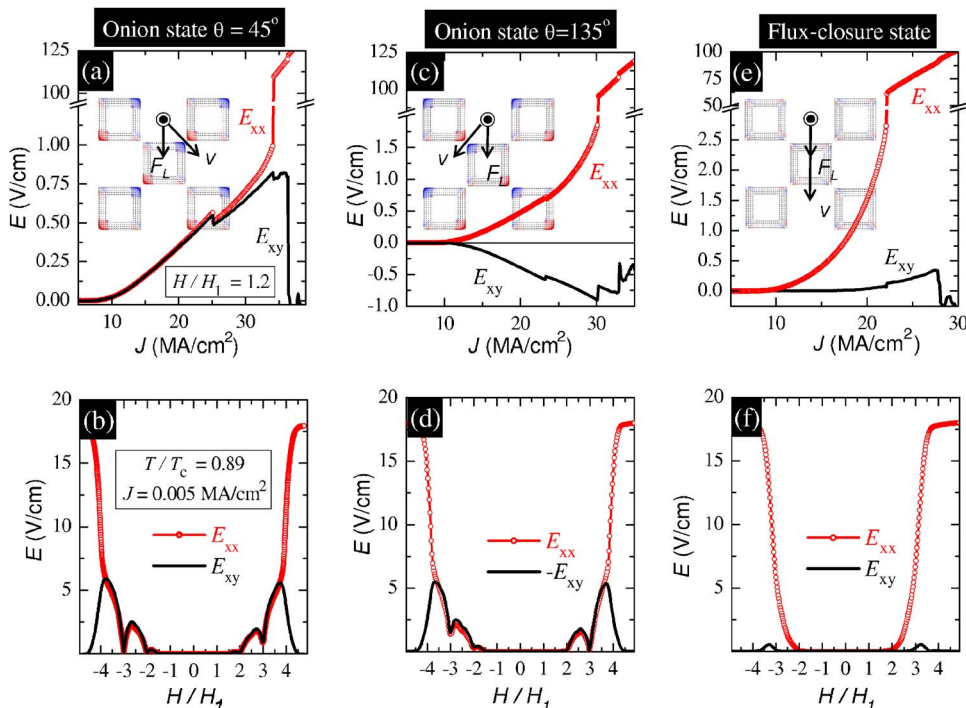


FIG. 2. (Color online) Parallel (E_{xx}) and transverse (E_{xy}) electric fields as a function of current density J (upper row) and field (lower row) at $T/T_c = 0.89$. The first column [panels (a) and (b)] corresponds to the square rings magnetized at 45° , as indicated in the inset of panel (a). The second column [panels (c) and (d)] presents the data for the square rings magnetized at 135° , as indicated in the inset of panel (c). The third column [panels (e) and (f)] corresponds to the squares in the flux-closure state, as indicated in the inset of panel (e).

dynamic behaviors, as shown in Fig. 2(b). For the low current density $J=0.005$ MA/cm² vortices remain pinned up to a field $H/H_1 \sim 1.5$ where the vortex-vortex interaction becomes stronger than the vortex-pinning interaction. At higher fields clear commensurability effects can be seen for $H/H_1 = 2$ and $H/H_1 = 3$. In this field region ($H/H_1 < 4$) the fact that $E_{xx} \approx E_{xy}$ indicates that vortices are guided by the pinning potential as described above. Eventually, for fields close to the upper critical field ($H/H_1 > 4$) the pinning potential weakens and the guided motion is suppressed.

These findings clearly demonstrate that the vortex motion can be effectively guided along the principal axes of the underlying pinning potential, but tell us little about the origin of this pinning potential. In other words, it is necessary to find out whether the guided vortex motion (GVM) results from the magnetic field distribution or from the corrugation of the superconducting film deposited on top of the squares. In order to answer this question we magnetized the square rings with an in-plane field 135° away from the current direction (0°), as shown in the inset of Fig. 2(c). In this way the topographic pinning remains the same whereas the magnetic pinning is rotated 90° with respect to the previous one. If the magnetic field distribution is responsible for the GVM then a channeling along the -45° direction with respect to \mathbf{F}_L should be detected. This is in agreement with the results shown in Figs. 2(c) and 2(d), where E_{xx} remains unchanged while E_{xy} reverses sign. The most convincing evidence, however, comes from panels (e) and (f) corresponding to the square rings in the flux-closure state. In this case the stray field generated by the domain walls in each square ring is strongly reduced and just a minor influence on the vortex dynamics is expected. This is indeed corroborated by the lack of guided motion as is evidenced by the condition $E_{xx} \gg E_{xy}$.¹⁶

In order to understand the origin of the GVM let us first hypothetically separate the different contributions arising from the lattice symmetry and from the local symmetry of the dipoles. This is schematically illustrated in Fig. 1(b). The lattice symmetry contribution can be obtained by assuming that each dipole behaves as an effective isotropic pinning center, very much like a lattice of circular holes. In this case it has been previously shown⁴ that the minimum pinning force is along the principal axes of the pinning lattice [broken line in Fig. 1(b)]. On the other hand, ignoring the presence of the lattice and just considering the pinning force acting on a test vortex located at a magnetic pinning site, gives rise to a strongly anisotropic pinning force¹⁷ [schematically displayed as an off-centered circle in Fig. 1(b)]. The thick solid line in Fig. 1(b) shows the resulting pinning force combining both effects: the fourfold symmetric lattice contribution and the nonsymmetric local magnetic field. It is clear from this analysis that the presence of the nonsymmetric magnetic field distribution lifts the degeneracy expected for the vortex channeling, as experimentally observed.

It should be emphasized that although the above description helps to identify the basic mechanisms behind the guided motion of vortices, it is derived from the unphysical assumption that magnetic and nonmagnetic contributions are separable. However, since the ultimate reason for vortex channeling lies on symmetry considerations, this effect should be independent of the particular functional form of the pinning force. It is worth mentioning that previous calculations within the London model are not adequate to verify

the present experiments since the average distance between vortices is comparable to the superconducting coherence length and therefore vortex core overlap cannot be neglected. Instead, more rigorous calculations within the Ginzburg–Landau formalism should be used.

In summary, we have reported experimental evidence indicating that the anisotropic potential landscape of a square array of magnetic dipoles is capable of directing the vortex motion 45° away from the driving force direction. The multiple states of the used magnetic rings allow us to switch this direction ($\pm 45^\circ$ for two different dipolar states and 0° for the flux-closure state) resulting in a control of the transverse voltage signal.

This work was supported by the Fund for Scientific Research-Flanders FWO-Vlaanderen, the Belgian Inter-University Attraction Poles IAP, the Research Fund K.U. Leuven GOA/2004/02, the European ESF NES programs, U.S. NSF Grant No. ECS-0202780, and CNM ANL Grants Nos. 468 and 470. A.V.S. is grateful for the support from the FWO-Vlaanderen. We acknowledge useful discussions with C. C. Souza Silva and G. Carneiro.

¹B. Y. Zhu, F. Marchesoni, and F. Nori, *Physica E (Amsterdam)* **18**, 318 (2003); *Phys. Rev. Lett.* **92**, 180602 (2004).

²A. T. Fiory, A. F. Hebard, and S. Somekh, *Appl. Phys. Lett.* **32**, 73 (1978); M. Baert, V. V. Metlushko, R. Jonckheere, V. V. Moshchalkov, and Y. Bruynseraede, *Phys. Rev. Lett.* **74**, 3269 (1995); J. I. Martín, M. Velez, J. Nogués, and I. K. Schuller, *ibid.* **79**, 1929 (1997).

³M. Lange, M. J. Van Bael, Y. Bruynseraede, and V. V. Moshchalkov, *Phys. Rev. Lett.* **90**, 197006 (2003); W. Gillijns, A. V. Silhanek, and V. V. Moshchalkov, *Phys. Rev. B* **74**, 220509(R) (2006).

⁴P. Martinoli, *Phys. Rev. B* **17**, 1175 (1978); H. Pastoriza, S. Candia, and G. Nieva, *Phys. Rev. Lett.* **83**, 1026 (1999); A. V. Silhanek, L. Van Look, S. Raedts, R. Jonckheere, and V. V. Moshchalkov, *Phys. Rev. B* **68**, 214504 (2003) and references therein; J. E. Villegas, E. M. Gonzalez, M. I. Montero, I. K. Schuller, and J. L. Vicent, *J. Phys. Chem. Solids* **67**, 482 (2006); V. Vlasko-Vlasov, U. Welp, G. Karapetrov, V. Novosad, D. Rosenmann, M. Iavarone, A. Belkin, and W.-K. Kwok, *Phys. Rev. B* **77**, 134518 (2008).

⁵J. E. Villegas, S. Savel'ev, F. Nori, E. M. Gonzalez, J. V. Anguita, R. Garcia, and J. L. Vicent, *Science* **302**, 1188 (2003); C. C. de Souza Silva, J. V. de Vondel, M. Morelle, and V. V. Moshchalkov, *Nature (London)* **440**, 651 (2006).

⁶R. Wordenweber, P. Lahl, and P. Dymashevski, *Physica C* **369**, 141 (2002).

⁷P. Selders and R. Wordenweber, *Appl. Phys. Lett.* **76**, 3277 (2000).

⁸S. Savel'ev, V. Yampol'skii, A. Rakhmanov, and F. Nori, *Phys. Rev. B* **72**, 144515 (2005).

⁹H. Takeda, K. Yoshino, and A. A. Zakhidov, *Phys. Rev. B* **70**, 085109 (2004).

¹⁰Q. Lu, C. J. Olson Reichhardt, and C. Reichhardt, *Phys. Rev. B* **75**, 054502 (2007); A. V. Silhanek, W. Gillijns, V. V. Moshchalkov, V. Metlushko, F. Gozzini, B. Ilic, W. C. Uhlig, and J. Unguris, *Appl. Phys. Lett.* **90**, 182501 (2007); W. Gillijns, A. V. Silhanek, V. V. Moshchalkov, C. J. Olson Reichhardt, and C. Reichhardt, *Phys. Rev. Lett.* **99**, 247002 (2007).

¹¹This thickness proves to be sufficient as T_c of the Al film on top of the as-grown magnets differs by less than 1% from T_c of a coevaporated reference film.

¹²A. Imre, E. Varga, L. L. Ji, B. Ilic, V. Metlushko, G. Csaba, A. Orlov, G. H. Bernstein, and W. Porod, *IEEE Trans. Magn.* **42**, 3641 (2006).

¹³X. B. Zhu, P. Grutter, V. Metlushko, and B. Ilic, *J. Appl. Phys.* **93**, 7059 (2003).

¹⁴P. Vavassori, M. Grimsditch, V. Novosad, V. Metlushko, and B. Ilic, *Phys. Rev. B* **67**, 134429 (2003).

¹⁵A. V. Silhanek, W. Gillijns, V. V. Moshchalkov, V. Metlushko, and B. Ilic, *Appl. Phys. Lett.* **89**, 182505 (2006).

¹⁶The small but finite transverse field observed when the rings are set in the flux-closure state results from the fact that not all the rings switch to that state but a minority remains in the dipolar state.

¹⁷G. Carneiro, *Phys. Rev. B* **72**, 144514 (2005); *Physica C* **432**, 206 (2005).